

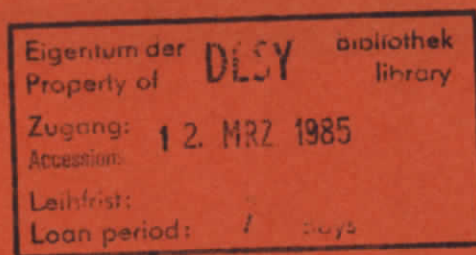
OSCILLATORY STRUCTURES IN BOUND-FREE FLUORESCENCE SPECTRA

OF Xe₂, Kr₂, and Ar₂

by

T. Möller, J. Stapelfeldt, M. Beland and G. Zimmerer

II. Institut f. Experimentalphysik, Universität Hamburg



ISSN 0723-7979

DESY behält sich alle Rechte für den Fall der Schutzrechtserteilung und für die wirtschaftliche Verwertung der in diesem Bericht enthaltenen Informationen vor.

DESY reserves all rights for commercial use of information included in this report, especially in case of filing application for or grant of patents.

To be sure that your preprints are promptly included in the
HIGH ENERGY PHYSICS INDEX ,
send them to the following address (if possible by air mail) :

DESY
Bibliothek
Notkestrasse 85
2 Hamburg 52
Germany

OSCILLATORY STRUCTURES IN BOUND-FREE FLUORESCENCE SPECTRA OF Xe_2 , Kr_2 , and Ar_2

T. MÖLLER, J. STAPELFELDT, M. BELAND and G. ZIMMERER

II. Institut für Experimentalphysik, Universität Hamburg
D-2000 Hamburg 50, Fed. Rep. of Germany



ABSTRACT

Following state selective, pulsed synchrotron radiation excitation of Xe_2 , Kr_2 , and Ar_2 , in time-resolved fluorescence spectra oscillatory bound-free structures of the first continua were observed. The low energy onsets are assigned to $O_u^+ + X O_g^+$ transitions at the left turning point. Our results rule out earlier assignments of fluorescence features to the left turning point observed under e^- or α -particle excitations of Kr and Ar. The shift of the oscillatory structures with excitation energy clearly supports our assignment.

submitted to Chem. Phys. Letters

1. Introduction

During the last years, several theoretical and experimental investigations of the electronic structure of Xe_2 (1), Kr_2 (2) and Ar_2 (3) were carried out. Nevertheless, remarkable uncertainties concerning the potential curves even of the lowest excited states, O_u^+ and I_u exist. Due to the large equilibrium distance of the van der Waals ground state, in photo absorption the excited states are probed only at large internuclear distances (fig. 1). Fluorescence from the minima of the O_u^+ and I_u states (the so-called 2nd continua) allows an estimate of the binding energies.

A necessary and very helpful source of information for the determination of the potential curves is the fluorescence from the inner part of the excited state to the strongly repulsive ground state (emission at "the left turning point", which is indicated in fig. 1). In the past, a few results were published about this type of fluorescence (4 - 9), but the correct assignment of the observed bands was controversy up to now.

In the present study, the fluorescence from the "left turning point" of the O_u^+ state of Xe_2 , Kr_2 , and Ar_2 was analysed in time-resolved experiments under spectrally selective, pulsed excitation with synchrotron radiation. The characteristic oscillatory structures of the bound-free transitions (10) were observed. This enabled us to assign unambiguously the low energy onset of this type of fluorescence to transitions at "the left turning point".

2. Experiment

The measurements were carried out at the experimental station Superlumi at HASYLAB, Hamburg. The entire set-up has been described previously (11,12). Spectrally selected synchrotron radiation with a band pass of .25 nm was used to excite the gases in a LiF gas cell. The fluorescence was analysed by a toroidal grating VUV monochromator with a band pass of 2nm. The pulsed structure of the exciting light (fwhm = 130 ps, repetition rate = 1 MHz) was exploited to provide time resolved data. The light was detected with a CsTe solar blind photomultiplier (Hamamatsu R 1460). The single photon counting technique was used.

The detection of the oscillatory structures of the 1st continua of rare gas molecules is difficult for the following reason. It requires direct $X O_g^+ \rightarrow O_u^+$ excitation of ground state molecules in the red, molecular wings of the resonance lines of the atoms. The equilibrium concentration, n_D , of ground state molecules is roughly proportional to the square of gas pressure, p (1). In order to deposit sufficient excitation energy in the gas to perform the experiment, p should be high. Note, that for Xe, at room temperature, $n_D \approx 0.006 \times n_{xe}$ at $n_{xe} = 2.7 \times 10^{19}$ atoms/cm³ (1). On the other hand, at high p , collisions destroy the initial vibrational population of the selectively excited molecules by vibrational relaxation and collisionally induced intersystem crossing $O_u^+ \rightarrow I_u$. Therefore, at high p , the steady state spectral distribution of fluorescence is a superposition of emission of various vibrational levels both of the O_u^+ and the I_u state, and the oscillatory structures are smeared out. In fig. 2, we present a typical steady state spectrum of Kr₂ ($p = 200$ torr, excitation wavelength $\lambda_{ex} = 125$ nm). It is in good agreement with previously reported results and contains emission from high vibrational levels (peak at 125 nm) and from vibrationally relaxed molecules (2nd continuum at 145 nm).

The problem can be overcome if the emission is detected only within a time window, Δt , immediately following the excitation pulses (delay, $\delta t = 0$). It is obvious, that synchrotron radiation excitation with its sharp excitation pulses at a high repetition frequency is well suited to perform this type of time-resolved fluorescence spectra. In view of the problem under discussion, Δt should be of the order of the gas kinetic collision time. The insert in fig. 2 shows a decay curve of the 1st continuum of Kr₂ ($p = 200$ torr) excited with $\lambda_{ex} = 125$ nm. One clearly observes the fast O_u^+ decay and a slow contribution which is attributed to the I_u state. Fig. 2 also shows the spectral distri-

bution of fluorescence within the time window indicated in the insert. The drastic differences between the steady state and the time resolved spectrum are obvious. The spectrum recorded with the time window ($\Delta t = 1$ ns) looks like the 1st continuum measured at very low pressure conditions. In this scale, the long wavelength onset of the 1st continuum with its oscillations cannot be observed, because the intensity is less than 1 % of the short wavelength maximum.

For all the three rare gases, optimal parameters ($p, \Delta t$) for each excitation wavelength were determined in order to observe the oscillatory structures. The parameters are given in the presentation of the results. They always have to be regarded as a compromise between contradictory requirements.

3. Results and Discussion

3.1 Determination of the "left turning points"

Fig. 3 shows the long wavelength range of time-resolved fluorescence spectra ($\Delta t = 8$ ns, $\delta t = 0$ ns) of Kr_2 (0_u^+) in a scale strongly enhanced compared with fig. 2. The excitation wavelengths for the curves are given in the figure and range between 124 nm and 126.5 nm. The spectra clearly yield the main features of bound-free transitions at small internuclear distances to a strongly repulsive state, namely the oscillations (10) and a systematic shift of the onset with the excitation wavelength (4). Similar results were obtained for Xe_2 (fig. 4) and Ar_2 (fig. 5).

According to the semi-classical treatment of bound-free transitions to a strongly repulsive ground state (13), the wavelengths corresponding to 65 % of the intensity of the lowest energy maxima are the wavelengths, λ_{LTP} , of the vertical transitions at the left turning point (vertical transition energy E_{LTP}). The values were extracted from the measurements for each excitation wavelength. However, we are mainly interested in λ_{LTP} at the level of dissociation of the 0_u^+ state. Under primary resonant excitation of 3P_1 atoms (Xe: 147 nm, Kr: 123.6 nm, Ar: 106.6 nm) no oscillations are observed because the temporal behaviour is governed by the imprisonment lifetime of the atoms and complicated collision processes (14). In order to extract λ_{LTP} and E_{LTP} at the dissociation limit of the 0_u^+ state, the values for λ_{LTP} were plotted as a function of the respective excitation wavelengths. These plots were extrapolated to the excitation wavelengths of the 3P_1 atoms. The results are collected in table 1.

Under particle excitation (electrons, α -particles) of rare gases, near UV bands were observed by several authors, e.g., 220 nm and 270 nm for Xe_2 (15), 220 nm (6) and 245 nm (7) for Kr_2 , and 190 nm and 210 nm for Ar_2 (5). These bands are often ascribed to $0_u^+ \rightarrow X 0_g^+$ and $1_u \rightarrow X 0_g^+$ transitions at the "left turning point", too. The literature results for the 0_u^+ state are included in table 1.

We tried to observe these near UV bands under photon excitation. Within the sensitivity of the experiment, no evidence for these bands was found. We would like to point out that due to the gating techniques used, the signal-to-noise ratio is excellent and the sensitivity is by far high enough to reproduce the literature results. The absence of the near UV bands under primary selective photon excitation of 0_u^+ molecules leads to the conclusion, that these

fluorescence features are connected with the excitation process (ionizing radiation) but have nothing to do with transitions at the "left turning point" of the 0_u^+ and 1_u states.

In the case of Xe_2 , our results confirm the earlier measurements of Ducuit et al (4) who used an experimental technique similar to ours. The authors measured a very weak and fast decaying continuum near 200 nm which shifts towards shorter wavelengths with increasing excitation wavelength indicating a larger slope of the ground state compared with the excited state around r_{LTP} . The weak continuum was attributed to the envelope of the oscillatory bound-free transition at "the left turning point". The assignment was supported by quantum mechanical calculations of FC-factors. In our spectra, the oscillations are clearly resolved.

Concerning Kr_2 , in table 1 two literature values for 0_u^+ emission at "the left turning point" of the same group are given (6,7). Schmoranzler et al used e^- -excitation and observed different broad near UV features. The strongest maximum was found at 220 nm and originally ascribed to the left turning point (6). This assignment was revised recently (7) in view of our results (16).

The assignments of Lorents (5) concerning the near UV bands of Ar_2 can be ruled out, too. We are the first who observe the oscillatory bound-free structure and its direct correlation to the excitation wavelength. The case of Ar is a drastical demonstration of the sensitivity of the set-up, because the excitation wavelengths are within the cut-off region of the LiF windows of the gas cell used which leads to a strong reduction of the excitation intensity inside the gas cell.

Table 1 contains also theoretical results for λ_{LTP} at the 0_u^+ dissociation limit. A direct comparison is only possible in the case of Xe_2 , because Ermler et al (17) calculated both the excited and the ground state. For Kr_2 and Ar_2 , Gadea et al (2) and Castex et al (3) calculated only the excited state. We combined these results with the experimental ground states determined by Foreman et al (18) to deduce the theoretical values for λ_{LTP} . In order to demonstrate, how sensitive the knowledge of the ground state influences λ_{LTP} for a given excited state, in the case of Xe_2 we additionally combined the excited state potential curve (17) with different experimental ground state potential curves (18,19). In no case, a satisfactory agreement between theory and experiment was found.

From the experimental transition energies at the "left turning point", the internuclear distance, r_{LTP} , itself can be deduced. However, it is necessary to know the potential curve of the ground state. Whereas the O_g^+ ground states of rare gas molecules are well known in the region of the van der Waals minimum (1-3), the data in the strongly repulsive part of the potential curves seem to be not as well settled as at large internuclear distances. We chose the potentials of Foreman et al (18) which - from the point of view of the experimental method used - should be the most reliable data at short internuclear distances. In the case of Xe_2 which is discussed in more detail below, we also used the potential of Farrar et al (19) to evaluate r_{LTP} . The numerical results are given in table 1. Independent from the ground state potential used, the experimental r_{LTP} is larger than the theoretical one (Xe_2) indicating that the binding energy given by Ermler et al (17) is too high. The opposite is found for Kr_2 and Ar_2 .

More details concerning the O_u^+ potential curves can be deduced from computer simulations of our spectra (quantum mechanical FC-calculations). A precise knowledge of the spectral distribution of the emission of vibrationally relaxed O_u^+ molecules will be an essential, additional ingredient in the determination of the potential curves. Such measurements were carried out at high gas pressures. The fast gating techniques were used to separate the 2nd continuum of the O_u^+ states from that of the l_u states. The evaluations are in progress now.

3.2 Some remarks concerning the O_u^+ potential curve of Xe_2

In the case of Xe_2 , Lipson et al (21) recently reported on a laser induced fluorescence study from which they could extract very precise values for the well depth of the O_u^+ state ($D_e = 4446(7) \text{ cm}^{-1}$), $\omega_e' = 124.86(30) \text{ cm}^{-1}$ and $\omega_e x_e' = 0.937(3) \text{ cm}^{-1}$. They did not deduce a value of the equilibrium distance, r_e , of the O_u^+ state. Combining our result for r_{LTP} with the results of Lipson et al (21), in the Morse-potential approximation we are able to deduce the equilibrium distance, r_e , of the O_u^+ state (and of course the Morse parameter, β). In doing so, two Morse potential curves are deduced, based upon the two ground state curves (18,19). Both model potentials are not satisfactory. Therefore we omit to give the values of r_e and of β . The model potentials predict a transition energy of the 2nd continuum differing from our experimental result by $\sim 2\%$. Moreover, both do not reproduce satisfactorily the experimental results of Castex (1) for the outer part of the O_u^+ potential curve. It seems

to us that the Morse-potential approximation is not well suited to describe the O_u^+ potential curve of Xe_2 .

Acknowledgements

The authors would like to thank the staff of HASYLAB for the continuous support. Numerous discussions with Dr. M.C. Castex, Paris, are gratefully acknowledged. The work was supported by the Bundesministerium für Forschung und Technologie (BMFT).

Table 1

Compilation of fluorescence wavelengths, λ_{LTP} (in nm), and of internuclear distances, r_{LTP} (in Å), at the left turning point of rare gas dimer O_u^+ states at the dissociation limit

	Xe ₂	Kr ₂	Ar ₂
λ_{LTP} (this work)	211	181	160
λ_{LTP} (other experiments)	214 (14)	220 (6) 178 (7)	190 (5)
λ_{LTP} (calculated)	238 (17) 227 (17)* >500 (17)**	142 (2)*	138.5 (3)*
r_{LTP} (this work)	2.63* 2.83**	2.27*	1.99*
r_{LTP} (theory)	2.58 (17)	2.53 (2)	2.1 (3) 2.2 (20)

* combined with the experimental ground state of ref. (18)

** combined with the experimental ground state of ref. (19)

References

- (1) M.C. Castex, J. Chem. Phys. 74, 759 (1981) and references therein
- (2) X. Gadea, F. Spiegelmann, M.C. Castex, and M. Morlais, J. Chem. Phys. 78, 7270 (1983) and references therein
- (3) M.C. Castex, M. Morlais, F. Spiegelmann, and J.P. Malrieu, J. Chem. Phys. 75, 5006 (1981) and references therein
- (4) O. Dutuit, M.C. Castex, J. LeCalvé, and M. Lavollée, J. Chem. Phys. 73, 3107 (1980)
- (5) D.C. Lorents, Physica 82C, 19 (1976)
- (6) K. Barzen, P. Wollenweber and H. Schmoranzler, Abstracts 13th ICPEAC (Eds. J. Eichler et al, Berlin 1983), p. 340
- (7) H. Schmoranzler, K. Barzen and P. Wollenweber, Abstracts 7th Internat. Conf. Spectral Line Shapes (Ed. F. Rostas, Aussois 1984), F 19
- (8) E.T. Verkhotseva, E.A. Katrunova, A.E. Ovechkin and Ya.M. Fogel', Chem. Phys. Lett. 50, 463 (1977)
- (9) G.N. Gerasimov and B.E. Krylov, Opt. Spectrosc. 55, 587 (1983)
- (10) M. Kraus and F.H. Mies, in "Excimer Lasers" (Ed. Ch. K. Rhodes), vol. 30 of Topics in Applied Physics (Springer, Berlin 1979), p. 5
- (11) H. Wilcke, W. Böhmer, R. Haensel and N. Schwentner, Nucl. Instr. Methods 208, 59 (1983)
- (12) P. Gürtler, E. Roick, G. Zimmerer and M. Fouey Nucl. Instr. Methods 208, 835 (1983)
- (13) R.J. Bieniek and T.J. Streeter, Phys. Rev. A 28, 3328 (1983)
- (14) H.D. Wenck, S.S. Hasnain, M.M. Nikitin, K. Sommer, G. Zimmerer and D. Haaks, Chem. Phys. Lett. 66, 138 (1979)
- (15) P. Millet, A. Birot, H. Brunet, J. Galy, B. Pons-Germain, and J.L. Teyssier, J. Chem. Phys. 69, 92 (1978)
- (16) T. Möller, J. Stapelfeldt and G. Zimmerer, Verhandl. DPG (VI) 19, 590 (1984)
- (17) W.C. Ermler, Y.S. Lee, K.S. Pitzer and N.W. Winter, J. Chem. Phys. 69, 976 (1978)
- (18) P.B. Foreman, A.B. Lees and P.K. Rol, unpublished results
- (19) J.M. Farrar, T.P. Schafer and Y.T. Lee, AIP Conf. Proc. 11, 279 (1973)
- (20) J.H. Yates, W.C. Ermler, N.W. Winter, P.A. Christiansen, Y.S. Lee and K.S. Pitzer, J. Chem. Phys. 79, 6145 (1983)
- (21) R.H. Lipson, P.E. LaRocque and B.P. Stoicheff, Opt. Lett. 9, 402 (1984)

Figure Captions

Fig. 1 An example for the O_g^+ ground state and the O_u^+ and 1_u excited states of a rare gas dimer. Given are theoretical results for Ar_2 [3,18]. The $O_g^+ \rightarrow O_u^+$ excitation is indicated by an arrow. The emission process at the "left turning point" is indicated, too, together with a calculated fluorescence spectrum with its oscillatory long wavelength onset.

Fig. 2 Fluorescence spectra of Kr_2 (Kr pressure 200 torr, excitation wavelength 125 nm). Curve 'a' is a steady-state (time-integrated) spectrum. Curve 'b' is a time-resolved spectrum (time window $\Delta t = 1$ ns, time delay to the excitation pulses $\delta t = 0$). The spectra are normalized at 125 nm. The insert shows a decay curve of Kr_2 fluorescence ($p = 200$ torr, $\lambda_{ex} = 125$ nm). The time window for time-resolved spectra is indicated schematically.

Fig. 3 Oscillatory long-wavelength range of $O_u^+ \rightarrow O_g^+$ time-resolved fluorescence of Kr_2 for different excitation wavelengths λ_{ex} . (Gas pressure $p = 100$ torr; time window $\Delta t = 8$ ns)

Fig. 4 Oscillatory long-wavelength range of $O_u^+ \rightarrow O_g^+$ time-resolved fluorescence of Xe_2 for different excitation wavelengths λ_{ex} . (Gas pressure $p = 100$ torr; time window $\Delta t = 4$ ns)

Fig. 5 Oscillatory long-wavelength range of $O_u^+ \rightarrow O_g^+$ time-resolved fluorescence of Ar_2 for different excitation wavelengths λ_{ex} . (Gas pressure $p = 200$ torr; time window $\Delta t = 5$ ns)

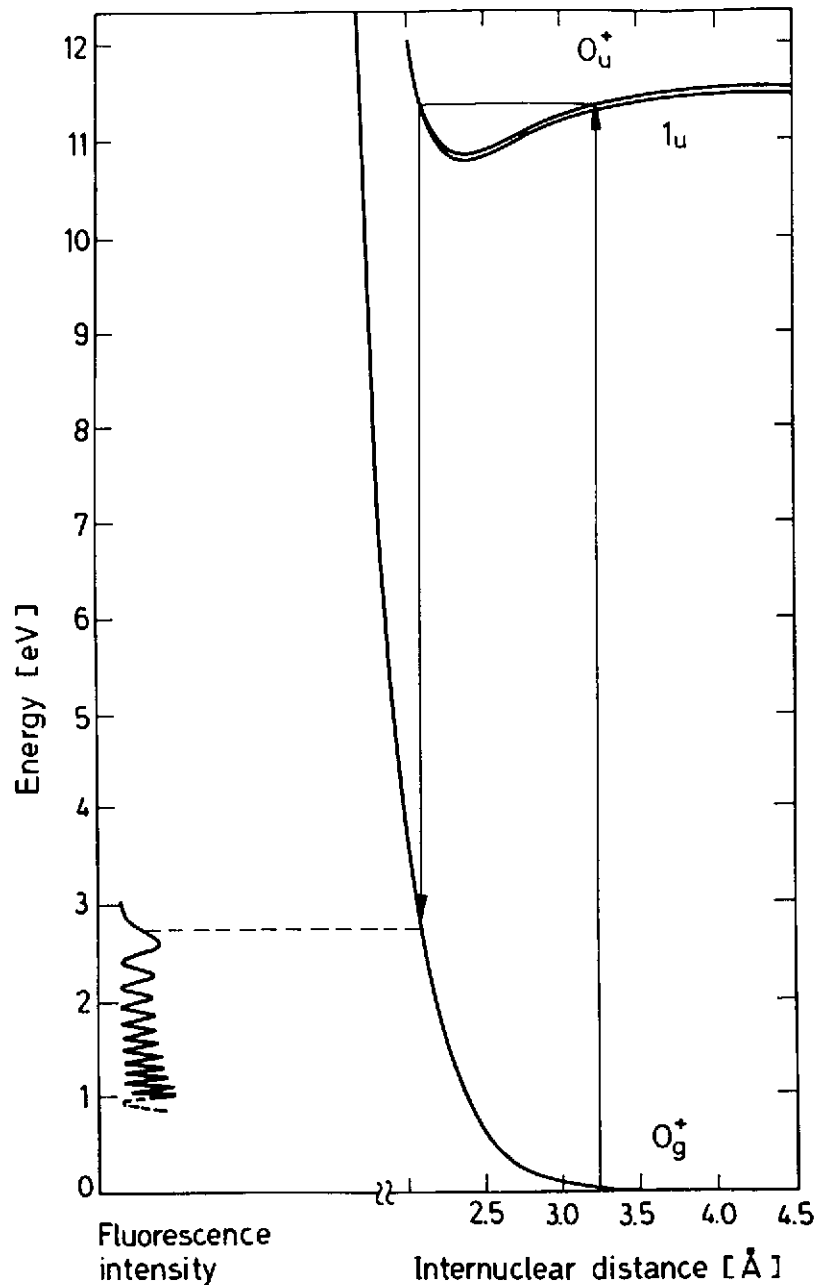


Fig. 1

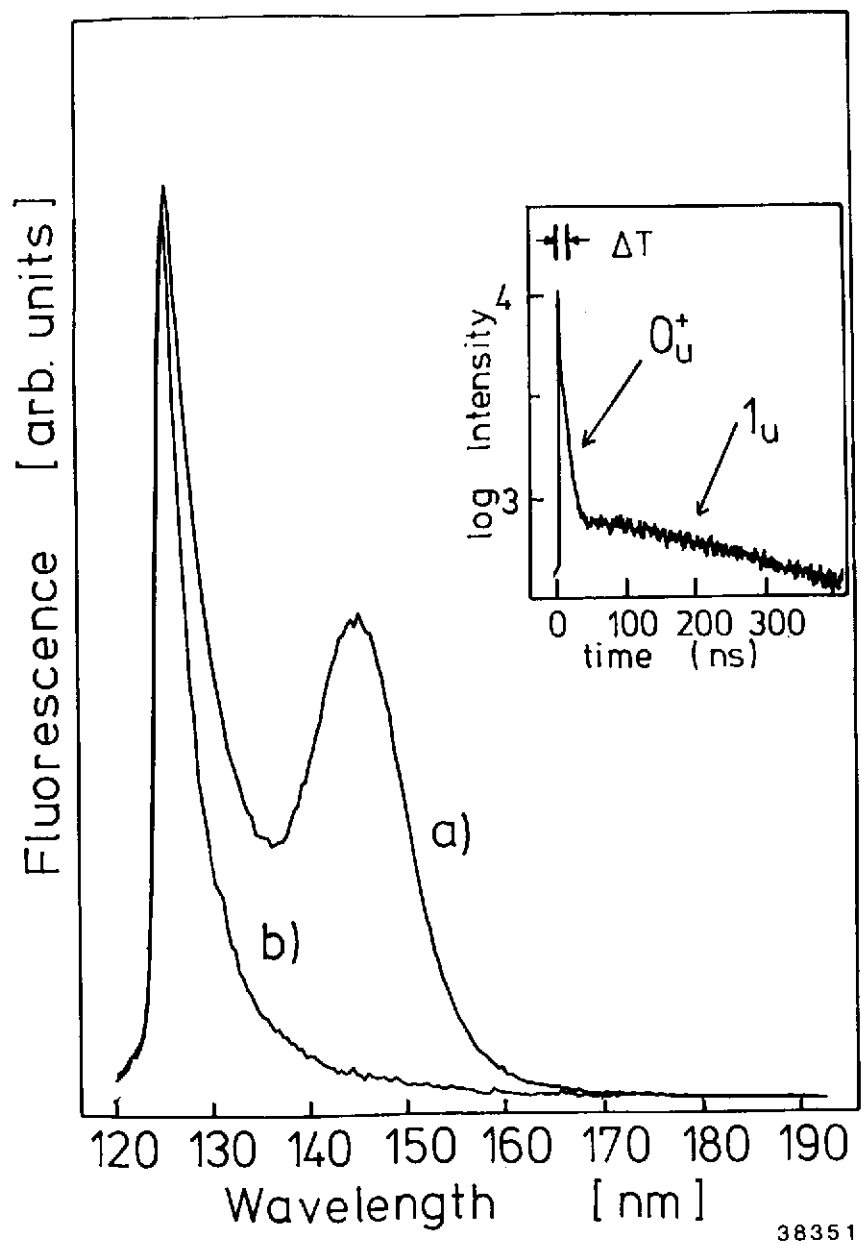


Fig. 2

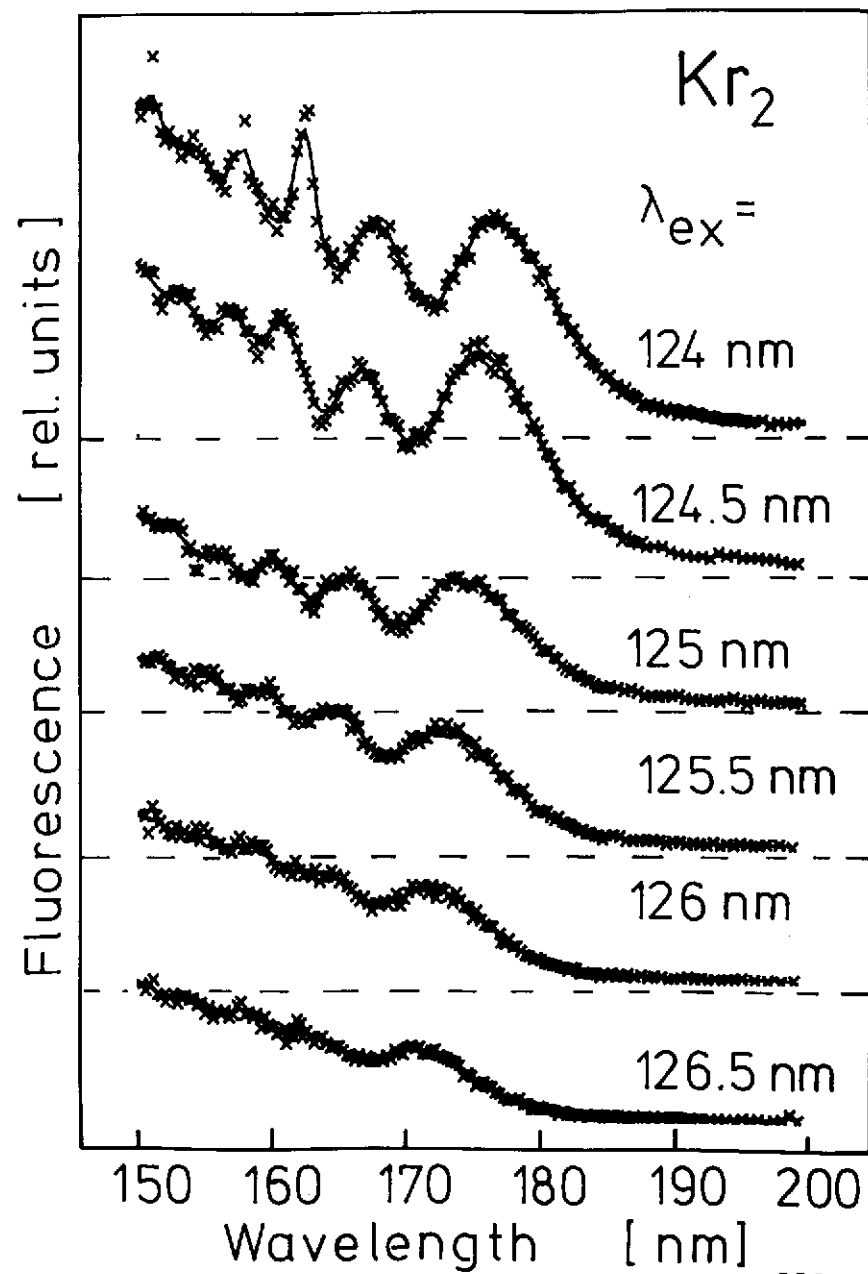
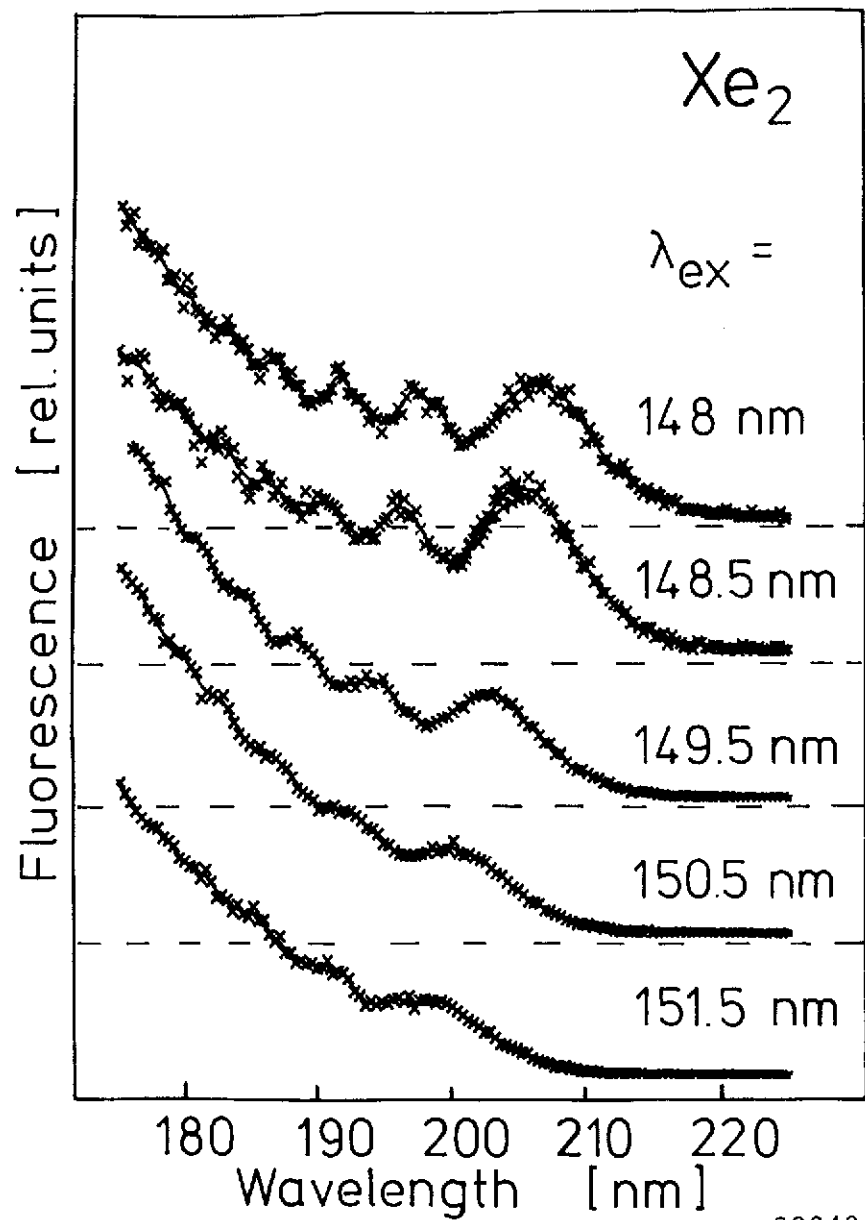
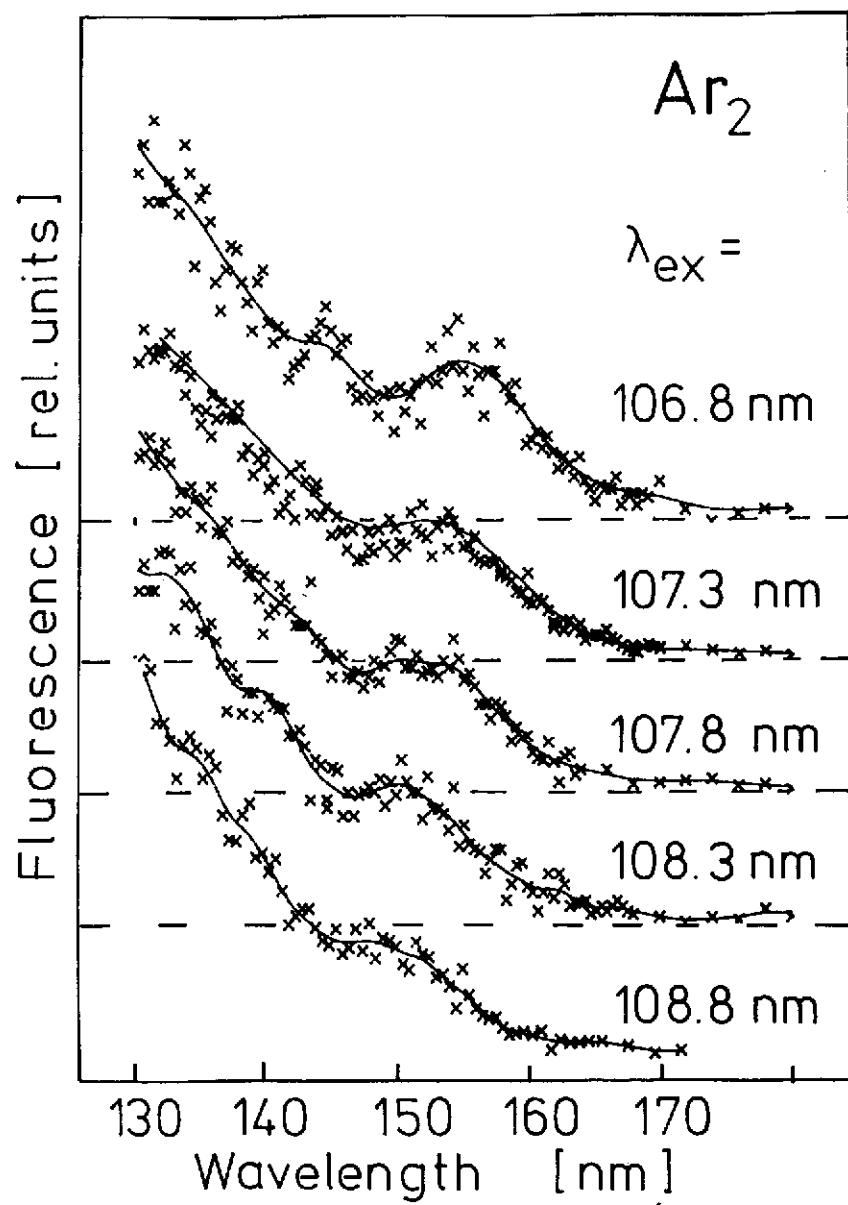


Fig. 3



38349

Fig. 4



38383

Fig. 5